Use of Dual Polarization Radar in Validation of Satellite Precipitation Measurements: Rationale and Opportunities

V. Chandrasekar[1], Arthur Hou[2], Eric Smith[2], V.N. Bringi[1], S.A. Rutledge[1], E. Gorgucci[3]

W.A. Petersen[4] and Gail Skofronick Jackson

[1]Colorado State University

[2]NASA Goddard Space Flight Center,
Greenbelt, MD

[3]Istituto di Scienze dell'Atmosfera e del Clima (CNR) Rome, Italy

[4]University of Alabama Huntsville

Corresponding author:

V. Chandrasekar,

Colorado State University

1373 Campus Delivery

Fort Collins, CO 80523-1373.

E-mail: chandra@engr.colostate.edu

Abstract

Dual-polarization weather radars have evolved significantly in the last three decades culminating in the operational deployment by the National Weather Service. In addition to operational applications in the weather service, dual-polarization radars have shown significant potential in contributing to the research fields of ground based remote sensing of rainfall microphysics, study of precipitation evolution and hydrometeor classification.. Furthermore the dual-polarization radars have also raised the awareness of radar system aspects such as calibration. Microphysical characterization of precipitation and quantitative precipitation estimation are important applications that are critical in the validation of satellite borne precipitation measurements and also serves as a valuable tool in algorithm development. This paper presents the important role played by dual-polarization radar in validating space borne precipitation measurements. Starting from a historical evolution, the various configurations of dual-polarization radar are presented. Examples of raindrop size distribution retrievals and hydrometeor type classification are discussed. The quantitative precipitation estimation is a product of direct relevance to space borne observations. During the TRMM program substantial advancement was made with ground based polarization radars specially collecting unique observations in the tropics which are noted. The scientific accomplishments of relevance to space borne measurements of precipitation are summarized. The potential of dual-polarization radars and opportunities in the era of global precipitation measurement mission is also discussed.

1. Introduction

Reliable global quantitative precipitation measurement is critically important for a variety of applications including flood forecasting, numerical weather prediction, understanding the evolution of hurricanes and severe storms, and tracking of long term trends in global precipitation and water supply. When combined with comprehensive ground validation and calibration, satellite observations offer practical prospects for acquiring accurate and global data sets especially over oceans and remote regions. Since the advent of satellite sensing of clouds and precipitation there has been much progress in terms of instrumentation and algorithm development.. The Tropical Rainfall Measuring Mission (TRMM), launched in 1997, represents a highly advanced active and passive remote sensing system to measure precipitation. Each precipitation satellite mission requires thorough ground validation to test instrument and algorithm performance . With the success of the TRMM mission and the plans for TRMM's successor mission the GPM, the current era represents the "golden age" of microwave precipitation sensing (National Academy press, 2007).

Yet, even with the success of TRMM, more complete coverage is needed, both spatially and temporally. TRMM only samples tropical precipitation ($\pm 35^{o}$ latitude) and has an orbit period of about 92 minutes and with an approximate repeat cycle of forty days (Chang et al 1999). Additional coverage is needed for short-term, fine-scale applications such as hydrology and for improving GCM models and validating such models. The committee on Earth Observing Satellites (CEOS) the international coordinating body for earth observing satellite systems (www.ceos.org) declared precipitation to be an important measurement and they identify TRMM's follow-on mission, the Global Precipitation Measurement (GPM) mission as a prototype of the Global Earth Observation System of Systems (GEOSS).

The GPM Mission is an international satellite mission to provide accurate precipitation measurements around the globe every 2 to 4 hours (http://gpm.gsfc.nasa.gov). The GPM mission concept is centered on the deployment of Core Observatory satellite with an active dual-frequency (Ka/Ku-band) precipitation radar and a passive GPM microwave imager (GMI) with wideband (10 - 183 GHz) capabilities. The core satellite will serve as a precipitation physics observatory and will provide the calibration standard for a constellation of dedicated and operational passive microwave sensors. The baseline GPM constellation is envisioned to comprise conically-scanning radiometers such as Global Microwave Imager (GMI), Global Change Observing Mission (GCOM) -W, Special Sensor Microwave Imager Sounder (SSMIS), supplemented by cross-track sounders such as Advanced Technology Microwave Sounder (ATMS) and Microwave Humidity Sensor (MHS) over land. GPM is currently a partnership between NASA and the Japan Aerospace Exploration Agency (JAXA), with opportunities for participation of additional partners via constellation satellites. The anticipated launch date of the GPM Core spacecraft is expected to be around 2013.

GPM is a science mission with integrated applications goals for advancing the knowledge of the global water/energy cycle variability as well as improving weather, climate, and hydrological prediction capabilities through more accurate and frequent measurements of global precipitation. The dual-frequency precipitation radar (DPR) aboard the GPM core satellite is expected to improve our knowledge of precipitation processes relative to the single-frequency radar used in TRMM by providing greater dynamic range, more detailed information on microphysics, and better accuracies in rainfall and liquid water content retrievals. The DPR will be able to provide information on the rain and snow distributions over a wide range of precipitation intensities (from ~0.2 to about 110 mm h^{-1}). This information will not only give us insight into

microphysical processes (evaporation, collision/coalescence, aggregation) but also provide bulk properties of the precipitation such as water flux (rain rate) and water content. The dual-frequency returns will also allow us to distinguish regions of liquid, frozen and mixed-phase precipitation. Overall, the combination of Ka and Ku bands should significantly improve the detection thresholds for light rain and snow relative to TRMM. The improved accuracy and more detailed microphysical information from the dual-wavelength radar can also be used to constrain the cloud model database to be used in simultaneous precipitation retrievals from the brightness temperature measurements by the multi-channel radiometer on the GPM Core. These radiometric improvements should be transferable to the constellation radiometers where simultaneous radar data are not be available.

Validation is an integral part of all satellite precipitation missions. The process of validation is a cross cutting effort covering many areas all the way from sensor development to ending with the end user products. Ground validation helps to characterize errors, quantify measurement uncertainty and most importantly, provide insight into the physical and statistical basis of the retrieval algorithms. The GPM validation falls in the general class of validation and integration of information from a variety of space borne observing platforms with ground-based measurements and data assimilation efforts. For TRMM, validation activity included elements such as, pointwise validation of space-borne radar measurements, statistical validation of the precipitation products, and validation for understanding precipitation processes. For GPM, the traditional approaches are planned with the addition of sites designed specifically to (1) perform statistical validation of retrieved satellite surface precipitation products, (2) investigate precipitation processes, and (3) to validate integrated hydrology applications.

Dual-polarization weather radar is a very powerful validation tool that can be used to address a number of important questions that arise in the validation process, especially those associated with precipitation microphysics and algorithm development. Right from the early introduction of circular polarization measurements by McCormick and Hendry (1975) and the subsequent advancement of linear polarization measurements by Seliga and Bringi (1976), polarization diversity radars have consistently advanced all three areas of interest for cross validation of space borne measurements namely, the understanding of precipitation processes, calibration and quantitative precipitation estimation. The introduction of differential phase measurements advanced the QPE applications (Seliga and Bringi 1978, Sachidananda and Zrnic, 1987, Chandrasekar et al 1990), whereas the microphysical characterization has advanced significantly to the level of producing hydrometeor classification products (Straka et al 2000, Liu and Chandrasekar, 1998, 2000 ; Vivekanandan et al 1999). The dual-polarization radar measurments were also used to advance the radar calibration for quantitative applications, using the self consistency principle of the polarization diversity measurements (Gorgucci et al 1992, Scarchilli et al 1996) Thus the dual-polarization measurements have played significant role in several areas of importance to cross-validation of satellite observation of precipitation.

The following describes the various aspects of the dual-polarization weather radar specifically in the context of validating space-borne precipitation estimates. This paper is organized as follows. Section 2 provides brief background on the dual-polarization weather radars, along with the discussion of various types of dual-polarization radar measurements. The different implementation of dual-polarization radars involves different technologies and they are also summarized. In section 3 the applications of dual polarization radars for rainfall microphysical research is reviewed specially in the context of space borne application. A brief

background of the TRMM program space based measurement of precipitation is discussed in section 4 along with the advancement made during the TRMM era in cross-validation of satellite measurements. The potential opportunities in the GPM era are summarized in section 5.

2. Historical evolution of dual polarization meteorological radars

The fundamental science of polarimetric radar observations of precipitation can be described by the diagram (in Fig. 1). The transmitted waveform propagates through precipitation media, is scattered back from the particles in the resolution volume, and after propagating back through precipitation media, is received by the radar. The propagation medium characteristics are described by the propagation matrix whereas the backscatter properties are described by the scattering matrix of precipitation resolution volume. The early pioneering work at the National Research Council (NRC) in Ottawa by McCormick, Hendry and colleagues focused on measuring the coherency matrix of precipitation at circular polarization (Bringi and Chandrasekar 2001). One of the major results that came out of the study was that they were not operating at the eigen-polarization states of the rain medium. The main implication was that, the polarization state keeps changing due to propagation through rain medium. This realization motivated the team led by Seliga and Bringi (1976) to operate at the eigen-polarization states of the rain medium, namely the horizontal (H) and vertical (V) states. In addition, for simplicity and hardware considerations they focused on an incomplete (but nevertheless microphysically relevant) set of measurements. Seliga and Bringi (1976) proposed two methods of obtaining polarization diversity measurements namely a) alternately switching the transmit polarization states between H and V polarization states, with copolar reception via a single receiver, and b) Simultaneous Transmit and Receive using dual channel receivers. (STAR-mode, according to

early CHILL radar acronym). The late seventies were prior to the digital revolution, and the alternate switching of polarization along with copolar signal reception with a single receiver was much cheaper to implement compared to the two-receiver mode of implementation. Subsequently many research radar installations upgraded their radars to dual-polarization capability including the NSF-CHILL radar, NCAR-CP-2, Chilbolton radar, and the Italian Polar 55-C. Most of the activities in the U.S were concentrated on making detailed copolar and cross-polar measurements and interpreting these data by developing simplified microphysical models.

In the mean time, in the late eighties the research team at German Aerospace Research Establishment (DLR) embarked on a fairly aggressive program to develop a polarization diversity radar to make measurements at arbitrary polarization states (Schroth et. al., 1988). They also installed a unique polarization switch-and-polarizer such that the receive polarization states could be controlled independent of the transmit polarization states. By then several teams including the DLR and Colorado State University CHILL (CSU-CHILL) started pursuing complete set of measurements from linear polarization states.

Though the initial NEXRAD radars were not dual polarized, polarization research initiated at National Severe Storm laboratory along with the overwhelming results from other radar installations mentioned above led to the deployment of a prototype dual-polarization radar for National Weather Service (Doviak et al. 2000). Similarly several European countries have initiated deployment of dual-polarization radars for operational applications indicating the maturity of the science and applications (Parent et al 2005). Thus, the dual-polarization radars have come a long way from early research to operational application. The Joint Polarization Experiment (JPOLE) conducted (Ryzhkov et al 2005, Zrnic and Ryzhkov 1999) evaluated the operational applications of Dual-polarization radar from a weather service perspective and

the potential demonstrated by the various observations of dual-polarization since the early eighties have resulted in a decision by the national Weather Service to upgrade the Weather Service Radars(WSR-88D) to dual-polarization. (www.roc.noaa.gov).

a) Dual polarization radar measurements

In a conventional single polarization radar the reflectivity factor is related to the back scatter cross-section of the individual precipitation particles through the particle size distribution. The various parameters measured from a dual-polarization radars are essentially the various elements of the dual-polarization covariance matrix (DPCV) of precipitation (Bringi and Chandrasekar, 2001). If a radar can measure all elements of the dual-polarization covariance matrix, then it is termed a fully polarimetric radar. Many dual-polarization radars measure only a subset of the elements of the dual-polarization covariance matrix (Bringi and Chandrasekar 2001). Most of the definitions of the various dual-polarization measurements are available in various research articles and textbooks (ex; Bringi and Chandrasekar 2001). The equivalent radar reflectivity factor is given by the diagonal elements of the covariance matrix, proportional to the volumetric radar cross section (Bringi and Chandrasekar 2001). An extension of this reflectivity measurement to dual-polarization with the distinction of radar cross section of particles and reflectivities between horizontal and vertical polarization states results in the differential reflectivity (Z_{dr}). Z_{dr} is defined as the ratio of reflectivities at horizontal and vertical polarization.

$$Z_{dr} = 10\log_{10}\left(\frac{Z_h}{Z_v}\right) \qquad (1)$$

Where Z_h, Z_v are the radar reflectivity factors measured at horizontal and vertical polarization. The co-polar correlation coefficient is defined as the correlation between the radar received signals at horizontal and vertical polarization , that is complex and has a magnitude between zero to one denoted by the symbol ρ_{co} , to indicate the copolar correlation coefficient.

In addition to measuring reflectivities at the same polarization state that was transmitted by the radar, the systems can be configured to measure the received power at the polarization state orthogonal to the transmit polarization state. This was routinely done at circular polarization operation (McCormick and Hendry, 1975), however not common with linear polarization states. When the cross polar power is measured at the linear polarization state then it is converted to an equivalent reflectivity factor and the ratio of copolar to cross polar reflectivity is termed as Linear Depolarization ratio (LDR). Z_h, Z_{dr} and LDR are real (power) measurements whereas ρ_{co} is complex, associated with magnitude and phase. As the electromagnetic wave from the radar propagates through precipitation, then the dual-polarization variables are modified due to propagation effects such as differential attenuation and differential phase between the H and V polarization states. At radar frequencies where the attenuation is negligible such as S-band, the main impact of propagation through precipitation is the differential phase. In the presence of propagation the phase of ρ_{co} is modified as:

$$Arg[\rho_{co}] = \Psi_{dp} = \phi_{dp} + \delta_{hv} \qquad (2)$$

The differential propagation phase (Φ_{dp}) is proportional to the water content along a rain path, and is one of the important parameters measured by dual-polarization radar (Jameson 1985). There are numerous articles in the literature that discuss the theory and applications of dual-polarization radar measurements and are summarized in the text book by Bringi and Chandrasekar (2001).

b) Configurations of dual-polarization radars

The term dual-polarization radar does not uniquely refer to a specific radar configuration or a set of measurements. Several configurations of dual-polarization radars are available depending on the measurement goals and choice of polarization states. The covariance matrix forms a complete set of measurements and several research radars are configured for this measurement. In the early 1980s a number of single polarized research radars were modified for limited dual polarization measurements in the linear horizontal/vertical polarization states, for measuring differential reflectivity and differential phase. These measurements involved only co-polar signals, and the system requirements were not very stringent (Wang and Chandrasekar, 2006) and significant practical results (such as rain rate estimation and hail detection) were obtained fairly quickly.

The most general dual-polarization radar can be described as the system that has both polarization-agility on transmit and polarization diversity on receive mode. Polarization agility refers to the ability to change the transmitted polarization state between any two orthogonal states on a pulse-to-pulse basis, whereas polarization diversity refers to the ability to simultaneously receive two orthogonal polarization states. Fig. 2 shows the generalized block diagram of a two-transmitter/two-receiver system that supports both polarization diversity and agility, enabling fully polarimetric measurements. The CSU-CHILL radar has this configuration at 10 cm wavelength (S-band) and more recently the similar configuration was implemented at the TRMM, GV facility at Okinawa (COBRA radar, Nakagawa et al. 2003). In addition, the various dual-polarization implementations at different installations can be broadly classified into

three types, namely, (1) polarization agile/single receiver systems, (2) polarization diversity systems, and (3) polarization agile dual-receiver systems. These types of systems have been described in detail in Bringi and Chandrasekar (2001).

3. Application of dual polarization radar to rainfall microphysical retrievals

a) Raindrop size distribution

Dual polarization radars have been used in retrieving Raindrop size distribution (DSD) parameters utilizing the relation between size and shape of raindrops. DSD is mainly used to describe the microphysical characteristics of the rain medium. The DSD also forms as the building block that is used to describe the remote sensing measurements of the rain medium.

The most important polarization diversity radar signatures of the rain medium from radars at low elevation angles are the differential reflectivity (Z_{dr}) and specific differential propagation phase (K_{dp}). These characteristic signatures are the consequence of the approximately oblate spheroidal raindrops coupled with a nearly vertical orientation of their symmetry axes forming an anisotropic propagation medium. The microphysical origin of these signatures is closely related to the raindrop size and shape distributions.

b) Raindrop shape

The equilibrium shape of a raindrop is determined by a balance of forces on the interface involving hydrostatic, surface tension and aerodynamic forces. Numerical model results of Beard and Chuang (1987) described the shape of raindrops as a function of size as shown in Fig. 3.

Wind tunnel data of Pruppacher and Beard (1970) yielded a simple approximation to the axis ratio of raindrops approximating the shape of oblate spheroids as

$$\frac{b}{a} = 1.03 - 0.062D, \qquad 1 \le D \le 9\ mm \tag{3}$$

Rotating linear polarization observations in rainfall showed that raindrops on the average fall with their symmetry axis along the vertical. Using the shape-size relation and the corresponding back scatter cross section of raindrops at horizontal and vertical polarization states, models of Z_{dr} and K_{dp} in rain have been developed to study the microphysics of rainfall from these measurements. The differential reflectivity measurement yields a good measure of the volume-weighted drop median diameter D_o. Similarly K_{dp} is proportional to the product of water content (W) and mass weighted mean diameter D_m (Jameson 1985; Bringi and Chandrasekar 2001). These intrinsic microphysical properties have been utilized extensively in the literature for various applications including retrieval of DSD parameters and rainfall estimation. Several laboratory experiments as well as measurements of free falling raindrops have essentially confirmed that the raindrop shapes are in the region suggested by Beard and Chuang (Chandrasekar et al. 1988; Kubesh and Beard 1993; Bringi et al. 1998; Andsager et al. 1999; Gorgucci et al. 2000; Thurai and Bringi 2005).

c) DSD retrievals

A long-standing pursuit of polarimetric radar applications has been the retrieval of raindrop size distribution. Early studies focused on the estimates of drop median diameter D_o or the mass-weighted mean diameter D_m. Fairly simple power law based retrievals have been developed in

the literature both based on theoretical considerations as well as empirical deductions (Seliga and Bringi, 1976; Aydin et al., 1987; Goddard and Cherry, 1984) of the form

$$D_o = a(Z_{dr})^b \tag{4}$$

The coefficients *a, b* depend on the frequency band at which the measurements are made. Thus it can be seen that dual-polarization measurements provide fairly simple retrievals of DSD parameters. Gorgucci et al. (2000) recognized that drop canting and oscillations could be incorporated into an "effective" drop shape parameter and proceeded to develop an algorithm to estimate the same from the radar measurement. It is important to recognize that even if drop axis ratio is in fact a non-linear function of D, it is possible to define an equivalent linear model such that the same relation between K_{dp}/N_w and D_o is preserved on average. Gorgucci et al. (2001, 2002) developed algorithms for retrieving rain rate (R) as well as D_o, N_w and μ using the effective shape concept in combination with the measurement pair (Z_h, Z_{dr}). The functional relationship between Z_{dr} and D_o is developed from the underlying microphysical relation between the mean axis ratio of raindrops and their size.

Once D_o is retrieved, then the other parameters of the DSD can be retrieved such as the intercept of the normalized form of a Gamma distribution (Gorgucci et al., 2002). The statistics of the parameter sets D_o, N_w are important in the development of algorithms. Bringi et al (2003) used the DSD retrieval method to scale the process to world wide application over different climatic regimes. While the above are parametric retrievals, non-parametric retrieval of DSDs are also possible combining the advantages of a Doppler and polarimetric radar as demonstrated by Moisseev and Chandrasekar (2006). Fig. 4 shows the nonparametric DSD retrieval from dual polarization spectral analysis.

The variability of the DSD across different climatic regimes can be demonstrated by examining the variability of mean $<N_w>$ versus mean $<D_m>$ where angle brackets denote averages. For example, Fig. 5a shows such data retrieved from disdrometer measurements as well as from polarimetric radar data for stratiform rain. A large extent of the data for Fig.5 came from the globally diverse ground validation observations of the TRMM program. For stratiform rain there appears to be a clear inverse relation between $log_{10}(<N_w>)$ and $<D_m>$; in fact, it is quite remarkable that a straight line fit results from the composite disdrometer and radar retrievals, these data encompassing a number of regimes from near equatorial to the US High Plains. From a microphysical perspective, stratiform rain results via the melting of snowflakes and/or tiny graupel or rimed particles. If the bright-band is "strong", then it likely reflects melting of larger, low-density and dry snowflakes into relatively larger raindrops, whereas if the bright-band is "weak" then it may reflect the melting of tiny, compact graupel or rimed snow particles (Waldvogel et al. 1995). In essence, the large, low density snowflakes lead to DSDs that have smaller $<N_w>$ and larger $<D_m>$ relative to the tiny, compact graupel or rimed snow particles.

Fig. 5b shows similar results for convective rain. There appears to be a cluster of data points with $<D_m>$=1.5-1.75 mm and $log_{10}<N_w>$=4-4.5, the regime varying from near equatorial (Papua New Guinea) to sub-tropics (Florida, Brazil) to oceanic (TOGA-COARE, Kwajalein, SCSMEX). This cluster may be referred to as a "maritime"-like cluster where rain DSDs are characterized by a higher concentration of smaller–sized drops. The Fort Collins flash-flood event is unusual for Colorado as the data fall in the "maritime"-like cluster. The vertical structure of reflectivity in this event was highly unusual for summer time Colorado storms resembling instead the vertical profile of Z in oceanic convection (Petersen et al 1999).

The second "cluster" is characterized by $<D_m>$=2-2.75mm and $log_{10}<N_w>$=3-3.5, the regime varying from the U.S. High Plains (Colorado) to continental (Graz, Austria) to sub-tropics (Sydney, Australia) to tropics (Arecibo, Puerto Rico). The "continental"-like cluster may be defined which reflects rain DSDs characterized by a lower concentration of larger-sized drops as compared with the previously-defined "maritime"-like cluster.

Rosenfeld and Ulbrich (2003) have elucidated on the microphysical mechanisms that contribute to systematic DSD differences using empirical *Z-R* relations obtained by many observers. Objective rain type classification has been proposed, among others, by L'Ecuyer et al (2004) using the 3-D structure of *Z* which is expected to reduce regime-dependent systematic errors in the rainfall estimates. A different way of classifying vertical profiles of *Z* is the method using self-organizing maps (SOM). The SOM is an unsupervised learning neural network that forms a non-linear mapping of vertical profile of *Z* to a two-dimensional map and has been applied to TRMM PR datasets on a global scale (Zafar and Chandrasekar 2004). However, the extent to which complex microphysical processes that ultimately lead to the DSD can be identified via only the 3D- or 1D-vertical structure of *Z*, though promising, is not as yet fully established. Polarimetric radars will play an important role in answering these questions.

d) Rainfall estimation and hydrometeor classification

The TRMM era has produced substantial progress in the understanding and application of dual-polarization radar observations of precipitation. The specific TRMM era deployments are discussed in section 4 whereas this section discusses the methodologies of dual-polarization radar rainfall estimation algorithms. The various dual-polarized radar measurement parameters

that are used in rainfall estimation are reflectivity (say at horizontal polarization Z_h), differential reflectivity (Z_{dr}), and specific differential propagation phase (K_{dp}) (Bringi and Chandrasekar 2001, Ryzhkov et al 2005). Numerous algorithms have been developed based on a combination of these three measurements. Z-R algorithms have been around for a long time, originally developed as statistical regression estimates between Z_h measured by radar and rainfall measured on the ground by gages. The concept of scaling and normalization of DSDs can be used to provide a physical basis for the Z-R relation. The Z-R algorithm is of the form

$$R = cZ^{\beta} \tag{5}$$

where the normalized DSD indicates that *c* is dependent on N_w whereas β is nearly constant.

Dual polarized radar measurements have been used to obtain algorithms for R, which can be generally classified as R(Z, Z_{dr}), R(K_{dp}) and R(K_{dp}, Z_{dr}) algorithms depending upon what variables are used in the estimation. Three classes can be defined depending on what combination of measurements they use such as R(Z, Z_{dr}), R(K_{dp}) and R(K_{dp}, Z_{dr}). The error structure of these algorithms have been analyzed extensively in the literature and summarized in Bringi and Chandrasekar (2001) and Ryzhkov et al (2005). Under ideal conditions of a perfectly calibrated radar and homogeneous resolution volume the error in these algorithms can be separated into error in the parameterization $\varepsilon_{p,}$ and the error due to measurement inaccuracy in radar observations, ε_m. The Z-R algorithms have large ε_p, whereas all dual-polarization algorithms have small parameterization error. The statement about ε_m is not so straightforward. The dual polarization algorithms yield the best estimates of rain rate for moderate-to-heavy rainfall. However, in light rain Z-R works fairly well provided the calibration state is accurately maintained (Chandrasekar et al. 1990, part 3). It is not useful to further define the performance of these algorithms without considering numerous other factors such as radar operating frequency,

sensitivity to calibration errors and contamination by ice hydrometeors. In addition to large parameterization errors, one of the major problems in reflectivity-based estimates is that any bias in the measurement such as those due to calibration errors or improper attenuation correction will go unnoticed until it becomes very large, of the order of 5 to 10 dB. Any such errors in the presence of dual-polarization radars will be recognized as inconsistencies in the "self consistency" of dual-polarization radar observations (Gorgucci et al. 1992; Scarchilli et al. 1996). The ability of dual-polarization radar observations that detect ice particles is also an advantage here, where simple reflectivity only radar may not be able to do the same. Thus even the simple reflectivity-based rainfall estimates will also benefit from dual-polarization radar observations. Thus, the renewed awareness of radar calibration brought along by the dual-polarization radar era is not surprising.

Apart from this, the measurements of K_{dp} and Z_{dr} have their own advantages. K_{dp} is obtained from only phase measurements, and they are completely immune to radar calibration problems (as opposed to reflectivity measurements). The advantage of K_{dp} in comparison to Z_h mirrors that of AM (amplitude modulation) versus FM (frequency or phase modulation). At the same time, similar to the problem of FM when the signal is weak, at low rainrates K_{dp} has large measurement errors. K_{dp} being a phase-based measurement has numerous advantages as enumerated in Zrnic and Ryzhkov (1996). Similarly, Z_{dr} is a relative power measurement and it can be calibrated to very high accuracy compared to reflectivity (Hubbert et al 2006). Thus K_{dp} and Z_{dr} based rainfall estimates are immune to absolute calibration errors. The recent article by Ryzhkov et al (2005) provides a summary of the evaluation done by the National Weather Service Prototype dual-polarization radar. Their evaluation showed that the polarimetric rainfall

algorithms tuned for the Joint Polarization Experiment (JPOLE) produced negligible bias as well as lower random error when compared to standard WSR 88D rainfall products.

All the above discussion pertains to pointwise rainfall estimate. The range cumulative differential phase does natural integration of K_{dp}. This feature lends itself to estimation of the area-integral of rainfall rate which can be estimated from direct differential phase measurements instead of having to compute K_{dp}. This technique to compute area-integrated of rainfall rate was introduced and evaluated by Raghavan and Chandrasekar (1994), Ryzhkov et al. (2000) and Bringi et al. (2001). These papers clearly demonstrate the advantage of dual-polarization measurements for rainfall estimation. The JPOLE results described in Ryshkov et al (2005) show similar advantages.

Numerous experiments have shown the improved estimates of dual-polarization rainfall estimates (Seliga et al. 1981; Aydin et al. 1995; Bringi et al. 2004; Ryzykov et al. 2005; Schuur et al. 2001); the best advantage has been demonstrated in extreme events such as a flash flood. The polarimetric radar estimates of the Fort Collins flash flood showed clearly that in extreme events the dual-polarization rainfall estimates perform very well (Petersen et al. 1999; Brandes et al. 1997). Fig. 6 shows the rainfall accumulation contours of $R(K_{dp}, Z_{dr})$, $R(Z_h, Z_{dr})$and NEXRAD Z-R compared against gage-based contours for the Fort Collins flash flood event. It can be clearly seen from Fig. 6 that the polarimetric radar algorithms gave the best estimate of rainfall.

In mid-latitudes, a direct application of the polarimetric radar algorithms has been difficult due to ice contamination. In order to account for this, hydrometeor classification and rainfall estimation have been applied together as a combined process to classify precipitation, before quantification. This philosophy has led to development of blended algorithms (Cifelli et al,

2005). As an example, Fig. 7 shows a time-series of rainfall over the location of the Urban Drainage and Flood Control District (UDFCD) ALERT rain gauge, located near Denver International Airport, on June 19, 2004. The time period shown extends from 15:47 local time (170.901 Julian day UTC) to 16:33 local time (170.942 Julian day UTC). The green line shows the actual rain gauge trace and the red and black lines represent rain rate estimates over the gauge using CHILL radar data in combination with the standard NEXRAD Z-R relationship (red line) and blended polarimetric algorithm as discussed above (black line). The latter method makes use of Z_{dr} and $K_{dp,}$ in addition to Z_h, in order to determine the optimum rainfall estimator at each grid point in the radar domain. The symbols represent the most probable hydrometeor-type in the radar volume over the location of the UDFCD rain gauge, based on hydrometeor classification: "R" represents rain and "WG" represents wet graupel. Note that the polarimetric algorithm does a much better job at reproducing the gauge estimate of rainfall, compared to the standard reflectivity-based technique. Because the blended algorithm utilizes differential phase and differential reflectivity information in addition to Z_h, it can detect the likely presence of precipitation ice (e.g, wet graupel) and adjust the rainfall retrieval algorithm to produce more reliable estimates of rainfall. In contrast, the non-polarimetric method cannot discriminate between ice particles and large raindrops and, in situation of mixed precipitation, can produce highly biased estimates of rainfall.

e) Hydrometeor Classification

Polarimetric radar measurements are sensitive to the types, shapes and size distributions as well as fall behaviors of hydrometeors in a radar resolution volume. As a result extensive

information about the microphysics of hydrometeors is contained in the polarization diversity radar measurements. The ability to classify hydrometeors has a wide variety of applications such as, initialization and validation of cloud microphysical models, choice of the right algorithm for precipitation estimation and evaluation of assumptions made in the precipitation retrieval processes. The mapping from polarimetric radar measurement space and hydrometeor type space is not one to one. Over the last two decades numerous advances have been made in the area of hydrometeor identification in specific storm types. Liu and Chandrasekar (1998, 2000) evaluated a variety of techniques such as decision tree, statistical decision theory, neural networks and fuzzy logic and presented arguments for synthesizing all the knowledge base of polarimetic radar measurements, using fuzzy logic to perform robust, hydrometeor classification. They also developed a fuzzy hydrometeor classification system and presented results from in-situ validation experiments using data from T-28 storm penetration aircraft and CSU-CHILL radar data. Vivekanandan et al. (1999) have presented synthesis of polarimetric radar measurement properties for hydrometeor classification. Straka et al. (2000) summarized microphysical properties of precipitation for hydrometeor classification. Since these early studies numerous researchers have reported advances in hydrometeor classification using polarimetric radar observations to the point it is becoming a fairly mature area of research. One of the major difference in application of hydrometeor classification for WSR-88D applications and space borne application is the emphasis on the full vertical structure of hydrometeor classification. The operational hydrometeor classification systems (Ryzhkov et al 2005, Keranen et al 2007) work on Plan Position Indicators (PPI) of dual polarization radar measurements. The space borne radar observation of precipitation has excellent vertical resolution, the cross validation with hydrometeor classification have focused more on ground based radar operation in Range Height

Indicator (RHI) mode. The RHI mode gets instantaneous vertical structure of dual polarization measurements in contrast to a reconstructed profile over a 5 minute volume scan. With such high resolution, Lim et al (2005) have been able to map the varying transition of the ice/water boundary as shown in Fig. 8. Such high resolution RHI scans and the corresponding hydrometeor classification are best suited for cross validation with space borne measurements. However the reconstructed volume scans can also be used if the cross validation can work with the reduced resolution of a reconstructed vertical profile from PPI volume scans. Currently there are two independently developed models for hydrometeor classification namely the CSU model and the NCAR/NSSL model. Though the basis principles of these models are similar, the two have developed with two underlying philosophies namely the CSU model separate the data quality and hydrometeor classification as separate processes whereas the NCAR/NSSL model combines them. Recently Lim et al. (2005) further developed CSU model striking a compromise between the properties of the original CSU model and NCAR/NSSL model, which essentially balances the metrics of probability of error and false positive classification. This new model also introduced the use of varying melting level information at hydrometeor classification process. The CSU model puts out fewer classes compared to the NCAR/NSSL model. Based on the arguments presented in Liu and Chandrasekar (2000) such as robustness, and simplicity of implementation and simplicity of adapting a common framework for regional and seasonal variabilities such as summer, winter, continental and oceanic fuzzy logic based hydrometeor classification scheme is becoming widely popular to the point that it is being applied to operational systems (Keranen et al 2007).

4. Progress on validation of TRMM precipitation measurement with dual polarization radars

The TRMM-PR records energy reflected from precipitation and surface targets. The PR is a 128-element active phased array system operating at 13.8 GHz. The PR electronically scans from right to left, looking in the flight direction across the ground track of the satellite every 0.6 seconds, with horizontal resolution at the ground of 4.3 km and a swath width of 215 km (Fig. 9).

Each PR scan contains 49 rays sampled over an angular sector of 34 degrees. For any given ray, the instrument begins recording samples at a fixed distance from the satellite and records a certain number of samples along the ray. The starting distance and the number of samples are different for each ray. Rays other than the nadir ray also sample below the ground surface. The purpose of this extension below the surface is to clearly detect the location of the surface. One of TRMM-PR's most important features is the ability to provide vertical profiles of rain and snow from the surface up to a height of about 20 km.

The PR is able to detect fairly light rain rates down to 0.7 mm/h. At intense rain rates, where the attenuation effects can be strong, new methods of processing have been developed that help correct for this effect. The Precipitation Radar is able to separate out rain echoes for vertical sample sizes of about 250 m when looking straight down. Data points in the vertical are saved in the normal sample. The mirror is contained in the normal sample. A subset of the remaining data points is saved in two oversamples: the surface oversample and the rain echo oversample. Both oversamples have a spacing of 250 m along a ray, but a region with both normal sample and oversample has a spacing of 125 m. The PR determines which levels to save in the oversamples based on its on-board determination of the surface bin. No data are saved as oversample in rays 1-10 and 40-49. Five levels are saved from rays 11-39 in the surface oversample. If the PR

detects the surface in an oversample bin, the surface oversample is centered on the detected surface. If, on the other hand, the PR detects the surface in a normal sample bin, 3 oversample bins are above and 2 oversample bins are below the detected surface. In addition, 28 levels (immediately above the surface oversample) are saved from rays 20-30 in the rain echo oversample. The TRMM-PR will carry out all these measurements while using only 224 watts of electric power. The TRMM satellite has a circular non-synchronous orbit with an altitude of approximately 350 km. This orbit allows the TRMM satellite to pass over each part of the surface of the earth at a different local time daily. Precipitation radar parameters are listed in Table 1.

Table 1. Precipitation radar parameters (adopted from PR Instruction Manual).

Radar Type	Active phased-array radar
Frequency	13.796 GHz and 13.802 GHz (Two-Channel frequency agility)
Swath Width	About 215 km
Observable Range	Over 20 km
Range Resolution	250 km
Horizontal Resolution	4.3 km (nadir)
Sensitivity	S/N per pulse ≥ 0 dB for 0.5 mm/h rain at rain top
Independent Samples	64
Data Rate	93.5 kbps
Weight	465 kg
Power	213 watts
Antenna Type	128-element slotted wave guide array antenna
Beam Width	0.71˚ x 0.71˚
Aperture	2.1 m x 2.1 m
Scan Angle	±17˚
Gain	About 47.4 dB
Transmitter Type	SSPA & LNA (128 channels)
Peak Power	Over 700 W
Pulse Width	1.6 μsec x 2 ch
Pulse Repetition Frequency	2776 Hz
Dynamic Range	About 81.5 dB

TRMM program operates many validation sites around the globe. In addition extensive field campaigns were also conducted. Among the validation sites the one in Darwin Australia has a C-band dual polarization radar (CPOL) for a long time. In addition, the CPOL radar was deployed during the South China Sea Monsoon Experiment, (SCSMEX). Substantial contribution to rain microphysics and rainfall algorithm were contributed by research and observations from this site. The impact of raindrop oscillations and K_{dp} based rainfall algorithm for tropics were

demonstrated fairly early from this site (Keenan et al. 1998). These concepts were further developed into fundamental contributions to rainfall microphysics. The CPOL data was also used to validate the rain-profiling algorithm developed for ground polarimetric radars. Among the other sites, the Texas Florida Under Flight-B (TEFLUN-B) and the Large Biosphere-Atmosphere Experiment (TRMM-LBA) both had full deployment of the National Center for Atmospheric Research, SPOL radar which is an S-band dual-polarization radar (Carey et al. 2001; Cifelli et al. 2004). Both deployments resulted in development of methodologies for interpretation of PR observations, evaluation of DSD assumptions, precipitation regime classification, validation of PR attenuation-correction algorithms, and area rainfall estimates. Nakagawa et al. (2004) presented similar application from the GV site in Okinawa.

In addition, a series of coordinated comparisons have been made between TRMM PR observations and ground polarimetric radar. Chandraskar et al (2003) conducted careful point-wise comparisons between TRMM PR and ground radar to show the potential of ground polarimetric radars to asses the attenuation correction process based on common data framework between ground radars and TRMM PR (Bolen and Chandrasekar 2003). Fig. 10 shows the schematic of comparing space borne and ground based radar observations. Fig. 11 shows a vertical profile comparison of the various parameters measured by the ground polarimetric radar such as reflectivity, differential reflectivity, LDR, and copolar correlation namely compared against the TRMM radar observations. Similar comparisons with C band polarimetric radars are shown in Fig. 12.

The normalized Gamma DSD model was used by Chandrasekar et al (2003) to conduct microphysical comparisons on a pixel basis from TRMM PR and ground polarimetric radar. Fig. 13 shows the inter-comparison of D_0 obtained from both TRMM PR and ground polarimetric

radars. The D_o retrieval algorithm were presented in their paper. This concept was extended to a global scale where global maps of DSD estimates were constructed in Chandrasekar et al (2005). This global map is a further scale-up of the DSD reported from different climatic region by Bringi et al (2003). Wilheit et al (2006) have shown the utility of such global maps for development of passive microwave remote sensing algorithms from satellite observations.

In summary, the limited use of dual-polarization radars during the TRMM era have yielded substantial benefits in numerous areas including a) validation of TRMM PR attenuation correction algorithms b) precipitation regime classification c) methodology for radar calibration and d) fundamental advances in understanding of rain microphysics in terms of differences between continental and oceanic events as well as convective and stratiform storms. These preliminary successes have led to development of the ground validation site at the Okinawa island of Japan, with a fully polarimetric C-band dual polarization radar.

5. *Pending opportunities for dual polarization radars in future precipitation such as GPM Missions*

Dual-polarization radars have undergone extensive evolution over the last two decades. The TRMM program has played a significant role in greatly expanding dual-polarization radar observations in the tropics. In fact TRMM is the only program that has embarked on deploying a dual-polarization radar in an open ocean environment. Combination of deployment in routine sites as well as in specialized field programs has expanded the knowledge base of rain microphysical properties. Several programs around the world are already pursuing dual-polarization upgrades such as WSR-88D program in the U.S, European Weather Radar Network and the ground radar network of Meteorological Service of Canada. Data quality and calibration

monitoring is one of the important attributes brought in by polarimetric radar that will be of great importance to satellite precipitation mission, specifically GPM. The potential of dual polarization radars to monitor the absolute calibration state has been discussed in numerous articles (Chandrasekar et al., 1990, part 3; Gorgucci et al., 1992 and the summary report, AMS workshop on radar calibration by Joe and Smith 2001).

The second area where dual-polarization radar provides great opportunity is in large scale cross-validation of microphysical properties of precipitation in the context of developing GPM era algorithms as well as validation of assumptions in satellite retrieval algorithms. The combination of DSD parameter retrievals and hydrometeor classification present tremendous opportunities for cross-validation. The distinction between water and ice (and mixed phase region) in the vertical structure of precipitation is likely to play a critical role in the development of both dual-frequency radar algorithms as well as combined radar-radiometer algorithms. This is one of the functions that dual-polarization radars are very good at, and will greatly benefit the GPM era algorithm development and validation.

The structure and lifecycle of precipitation is another important area of interest to global precipitation estimates. The ability of dual-polarization radars to monitor the microphysical evolution from early growth state, vigorous growth stage to a mature stage has been well documented in numerous experiments (Bringi and Chandrasekar 2001). This property of dual-polarization radars is useful in both radiative transfer modeling applications as well as cloud microphysical model validations. Both these areas namely cloud models and radiative transfer models play key roles in GPM thus making dual polarization radar a valuable analytic instrument (Wilheit et al 2006).

While GPM has not formalized GV plans, newer technologies and dual polarization and/or dual-frequency ground radars are sure to play an important role. Since GPM provides global precipitation estimate at 2-4 hour temporal resolution, international partners will play an important part in ground validation. GPM will need the capabilities of these informative ground instruments for satellite product evaluation. Further, ground radars serve a useful purpose in allowing for continuous monitoring of local precipitation events with great detailing of hydrometeor properties, thus allowing for microphysical process studies and storm evolution.

References

Andsager, K., K.V. Beard and N.F. Laird, 1999: Laboratory measurements of axis ratios for large raindrops. *J. Atmos. Sci*., **56**, 2673-2683.

Aydin K., V.N. Bringi and L. Liu, 1995: Rainrate estimation in the presence of hail using S-band specific differential phase and other radar parameters. *J. Appl. Meteor.,* **34**, 404-410.

Aydin, K., H. Direskeneli, and T. A. Seliga, 1987: Dual-polarization radar estimation of rainfall parameters compared with ground-based disdrometer measurements: October 29, 1982, Central Illinois experiment. *IEEE Trans. Geosci. Remote Sens.*, **GE-25**, 834-844.

Beard, K. V., and C. Chuang, 1987: A new model for the equilibrium shape of raindrops. *J. Atmos. Sci.,* **44,** 1509-1524.

Bolen, S.M. and V. Chandrasekar. 2003: Methodology for Aligning and Comparing Spaceborne Radar and Ground-Based Radar Observations. *J. Atmos. Oceanic Technol.*, **20**, 647–659.

Brandes, E.A., J. Vivekanandan, and J.W. Wilson, 1997: Radar rainfall estimates of the Buffalo Creek flash flood using WSR-88D and polarimetric radar data. Preprints, *28th Conf. on Radar Meteorology,* Austin, TX, Amer. Meteor. Soc., 123-124.

Bringi, V.N., V. Chandrasekar and R. Xiao, 1998: Raindrop axis ratios and size distributions in Florida rainshafts: An assessment of multiparameter radar algorithms. *IEEE Trans. Geosci. Remote Sens*., **36**, 703-715.

Bringi, V.N. and V. Chandrasekar, 2001: Polarimetric Doppler Weather Radar: Principles and Applications. *Cambridge University Press*.

Bringi, V.N., Gwo-Jong Huang, V. Chandrasekar and T. D. Keenan. 2001**:** An Areal Rainfall Estimator Using Differential Propagation Phase: Evaluation Using a C-Band Radar and a Dense Gauge Network in the Tropics. *J. Atmos. Oceanic Technol.*, **18**, 1810–1818.

Bringi, V.N., V. Chandrasekar, J. Hubbert, E. Gorgucci, W. L. Randeu and M. Schoenhuber, 2003: Raindrop Size Distribution in Different Climatic Regimes from Disdrometer and Dual-Polarized Radar Analysis. *J. Atmos. Sci.,* **2**, 354–365.

Bringi, V.N., Taiwen Tang and V. Chandrasekar. 2004: Evaluation of a New Polarimetrically Based *Z–R* Relation. *J. Atmos. Oceanic Technol.*, **21**, 612–623.

Carey L.D., R. Cifelli, W. A. Petersen, S. A. Rutledge, and M. A. F. Silva Dias 2001: Characteristics of Amazonian rain measured during TRMM-LBA. In *Preprints, 30th International Conference on Radar Meteorology*, July 18-24, Munich, Germany.

Chandrasekar, V., W.A. Cooper, and V.N. Bringi, 1988: Axis Ratios and Oscillations of Raindrops. *J. Atmos. Sci.* **45**, 1323–1333.

Chandrasekar, V., V.N. Bringi, N. Balakrishnan and D.S. Zrnic. 1990: Error Structure of Multiparameter Radar and Surface Measurements of Rainfall. Part III: Specific Differential Phase, *J. Atmos. Oceanic Technol.,* **7**, 621–629.

Chandrasekar, V., S.M. Bolen, E. Gorgucci, 2003: Microphysical cross validation of spaceborne radar and ground polarimetric radar**,** *IEEE Trans. Geosci. Remote Sensing,* **41**, 2153 – 2165.

Chandrasekar, V., W. Li, B. Zafar, 2005**:** Estimation of raindrop size distribution from spaceborne Radar observations, *IEEE Trans. Geosci. Remote Sensing,* **43**, 1078 – 1086.

Chang, A.T.C., L.S. Chiu, C. Kummerow, J. Meng, T.T. Wilheit, 1999: First results of the TRMM microwave imager (TMI) monthly oceanic rain rate: Comparison with SSM/I, *Geophys. Res. Lett.*, **26**, 2379–2382.

Cifelli, R., L. C. Carey, W. A. Petersen, and S. A. Rutledge, 2004: An ensemble study of wet-season convection in the South West Amazon: Kinematics and implications for diabatic heating, *J. Climate*, **17**, 4692–4707.

Cifelli, R., P. Kennedy, V. Chandrasekar, S. W. Nesbitt, S. A. Rutledge, and L. D. Carey, 2005: Polarimetric rainfall retrievals using blended algorithms, *32th Radar Meteorology Conference*, Albuquerque, NM.

Doviak R.J., V. Bringi, A. Ryzhkov, A. Zahrai and D. Zrnic, 2000: Considerations for Polarimetric Upgrades to Operational WSR-88D Radars, *J. Atmos. Oceanic Technol.,* **17**, 257–278.

Goddard, J.W.F. and S.M. Cherry, 1984: The ability of dual-polarization radar (copolar linear) to predict rainfall rate and microwave attenuation, *Radio Sci.*, **19**, 201-208.

Gorgucci, E., G. Scarchilli,, V. Chandrasekar, 1992: Calibration of radars using polarimetric techniques, *IEEE Trans. Geosci. Remote Sensing*, **30**, 853-858.

Gorgucci, E., G. Scarchilli, and V. Chandrasekar, 2000: Measurement of mean raindrop shape from polarimetric radar observations, *J. Atmos. Sci.,* **57**, 3406-3413.

Gorgucci E., G. Scarchilli, V. Chandrasekar and V.N. Bringi, 2001: Rainfall Estimation from Polarimetric Radar Measurements: Composite Algorithms Immune to Variability in Raindrop Shape–Size Relation, *J. Atmos. Oceanic Technol.,* **18**, 1773–1786.

Gorgucci, E., V. Chandrasekar, V.N. Bringi and G. Scarchilli, 2002: Estimation of Raindrop Size Distribution Parameters from Polarimetric Radar Measurements. *J. Atmos. Sci.,* **59**, 2373–2384.

Hubbert, J., F. Pratte, 2006: Differential reflectivity calibration for NEXRAD, *Proceedings, IGRASS06*, Denver, 2006.

Jameson, A.R. 1985: Microphysical interpretation of multi-parameter radar measurements in rain. Part III: Interpretation and measurement of propagation differential phase shift between orthogonal linear polarizations. *J. Atmos. Sci*., 42, 607-614.

Keenan, T., K. Glasson, F. Cummings, T. S. Bird, J. Keeler, J. Lutz, 1998: The BMRC/NCAR C-Band Polarimetric (C-POL) Radar System. *J. Atmos. Oceanic Technol.* **15**, 871–886.

Keranen, R., E. Saltikoff, V. Chandrasekar, S. Lim, J. Holmes, and J. Selzler, 2007: Real-time hydrometeor classification for the operational forecasting environment, *33th Radar Meteorology Conference*, Cairns, Australia.

Kubesh R.J. and K.V. Beard, 1993: Laboratory measurements of spontaneous oscillations for moderate-size raindrops. *J. Atmos. Sci.,* **50**, 1089-1098.

L'Ecuyer, T.S., C. Kummerow and W. Berg. 2004: Toward a Global Map of Raindrop Size Distributions. Part I: Rain-Type Classification and Its Implications for Validating Global Rainfall Products. *J. Hydrometeorology* **5**, 831–849.

Lim, S., V. Chandrasekar, and V.N. Bringi, 2005: Hydrometeor classification system using dual-polarization radar measurements: model improvements and in situ verification, *IEEE Trans. Geosci. Remote Sensing*, **43**, 792-801.

Liu H. and V. Chandrasekar, 1998: An adaptive neural network scheme for precipitation estimation from radar observations, *IGARSS'98*, **4**, 1895 – 1897.

Liu H. and V. Chandrasekar, 2000: Classification of Hydrometeors Based on Polarimetric Radar Measurements: Development of Fuzzy Logic and Neuro-Fuzzy Systems, and In Situ Verification. *J. Atmos. Oceanic Technol.,* **17**, 140–164.

McCormick, G. C., and A. Hendry, 1975: Principles for the radar determination of the polarization properties of precipitation. *Radio Sci.,* **10,** 421–434.

Moisseev, D.N., V. Chandrasekar and F. Junyent, 2006: Measurements of raindrop-size distributions from dual-polarization spectral observations. *Proc. ERAD 2006*, 18-22, September, Barcelona, Spain, 248-251.

Nakagawa, K., H. Hanado, S. Sato,and T. Iguchi, 2003: Development of the CRL Okinawa Bistatic Polarimetric Radar, *J. Communications Research Lab.*, 49, 225-231.

Nakagawa, K., H.Hanado, N. Takahashi, S. Satoh, T. Iguchi, K.Fukutani, 2004: Polarimetric rainfall observations with COBRA in the rainy season. *Fifth International Sympo. on Hydro. Appli. of Weather Radar*, 2-4 February, Melbourne, Australia.

Parent, J., P. Tabary and M. Guimera, 2005: The Panthere project and the evolution of the French operational radar network and products : rain-estimation, Doppler winds and dual-polarisation, *32th Radar Meteorology Conference*, Albuquerque, NM.

Petersen W.A., L.D. Carey, S.A. Rutledge, J.C. Knievel, R.H. Johnson, N.J. Doesken, T.B. McKee, T.V. Haar and J.F. Weaver, 1999: Mesoscale and Radar Observations of the Fort Collins Flash Flood of 28 July 1997. *Bull. American Meteor. Soc*., **80**, 191–216.

PR Instruction Manual (for Product Version 5) http://www.eorc.nasda.go.jp/TRMM/document/pr_manual/pr_manual2.pdf, 2004.

Pruppacher, H. R and K. V. Beard, 1970: A wind tunnel investigation of the internal circulation and shape of water drops falling at terminal velocity in air. *Quart. J. Roy. Meteor. Soc.,* **96,** 247-256.

Raghavan R. and V. Chandrasekar. 1994: Multiparameter Radar Study of Rainfall: Potential Application to Area–Time Integral Studies**.** *J. Appl. Meteor.*, **33**, 1636–1645.

Rosenfeld, D., and C. W. Ulbrich, 2003: Cloud microphysical properties, processes, and rainfall estimation opportunities. *Radar and Atmospheric Science: A Collection of Essays in Honor of David Atlas,* R. M. Wakimoto and R. Srivastava, Eds., Amer. Meteor. Soc., 237–258.

Ryzhkov A., D. Zrnic and R.Fulton, 2000: Areal Rainfall Estimates Using Differential Phase. *J. Appl. Meteor.*, **39**, 263–268.

Ryzhkov A.V., S.E. Giangrande and T.J. Schuur, 2005: Rainfall Estimation with a Polarimetric Prototype of WSR-88D. *J. Appl. Meteor.*, **44**, 502–515.

Sachidananda, M. and D.S. Zrnic, 1987: Rain Rate Estimates from Differential Polarization Measurements, *J. Atmos. Oceanic Technol.*, **4**, 588-598.

Scarchilli, G., E. Gorgucci, V. Chandrasekar, A. Dobaie, 1996: Self-consistency of polarization diversity measurement of rainfall. *IEEE Trans. Geosci. Remote Sensing*, **34**, 22–26.

Schroth, A., M. Chandra and P. Meischner, 1988: C-band coherent polarimetric radar for propagation and cloud physics research. *J. Atmos. Oceanic Technol.*, **5**, 803-822.

Schuur, T. J., A. V. Ryzhkov, D. S. Zrnic, and M. Schoenhuber, 2001: Drop size distributions measured by a 2D video disdrometer: Comparison with dual-polarization data. *J. Appl. Meteor.,* **40,** 1019–1034.

Seliga, T.A. and V.N. Bringi, 1976: Potential use of the radar reflectivity at orthogonal polarizations for measuring precipitation. *J. Appl. Meteor.,* **15,** 69-76.

Seliga, T.A. and V.N. Bringi, 1978: Differential reflectivity and differential phase shift: Applications in radar meteorology. *Radio Sci.,* **13,** 271-275.

Seliga, T.A., V.N. Bringi and H.H. Al-Khatib, 1981: A preliminary study of comparative measurement of rainfall rate using the differential reflectivity radar technique and a rainguage network. *J. Appl. Meteor.,* **20**, 1362-1368.

Straka J.M., D.S. Zrnic and A.V. Ryzhkov. 2000: Bulk Hydrometeor Classification and Quantification Using Polarimetric Radar Data: Synthesis of Relations, *J. Appl. Meteor.*, **39**, 1341–1372.

Thurai M. and V.N. Bringi, 2005: Drop Axis Ratios from a 2D Video Disdrometer, *J. Atmos. Oceanic Technol.*, **22**, 966–978.

Vivekanandan J., S. M. Ellis, R. Oye, D. S. Zrnic, A. V. Ryzhkov and J. Straka. 1999: Cloud Microphysics Retrieval Using S-band Dual-Polarization Radar Measurements, *Bull. American Meteor.l Soc.* **80**, 381–388.

Waldvogel, A., W. Henrich, W. Schmid, 1995: Raindrop size distributions and radar reflectivity profiles, *27th Radar Meteorology Conference*, Vail, CO., 26-28.

Wang Y. and V. Chandrasekar, 2006: Polarization isolation requirements for linear dual-polarization weather radar in simultaneous transmission mode of operation, . *IEEE Trans. Geosci. Remote Sensing,* **44**, 2019-2028.

Wilheit, T, V. Chandrasekar and W. Li., 2006: Impact of Uncertainty in the Drop Size Disatribution on Oceanic Retrievals from Passive Microwave Observations, *Proceedings, IGRASS06*, Denver, 2006.

Zafar, B.J. and V. Chandrasekar, 2004: SOM of space borne precipitation radar rain profiles on global scale, *Proceedings. IGARSS '04*, **2**, 925 – 928.

Zrnic D.S. and A. Ryzhkov, 1996: Advantages of Rain Measurements Using Specific Differential Phase. *J. Atmos. Oceanic Technol.,* **13**, 454–464.

Zrnic D.S. and A. Ryzhkov, 1999: Polarimetry for weather surveillance radars. *Bull. American Meteor.l Soc.*, 80, 389-406.

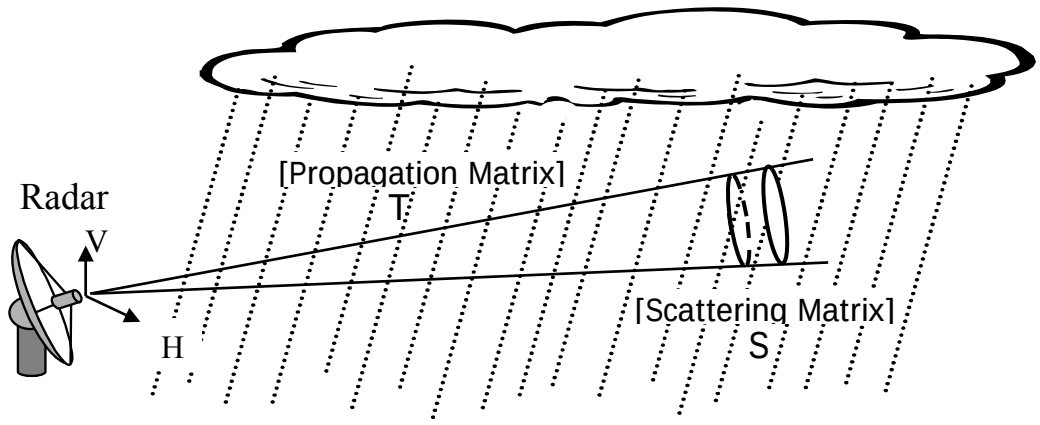

Fig. 1. Schematic of the propagation and backscatter in precipitation

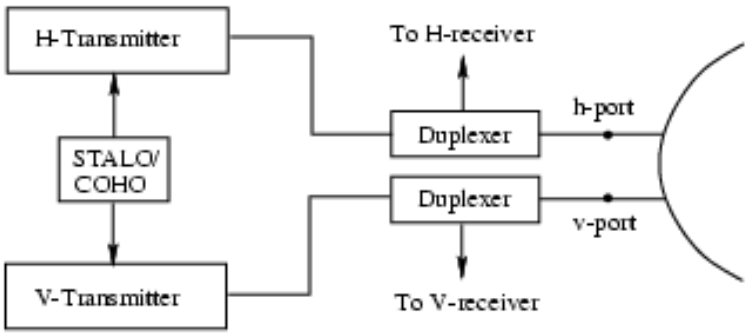

Fig. 2 Simple block diagram of the two-transmitter CSU-CHILL radar system.

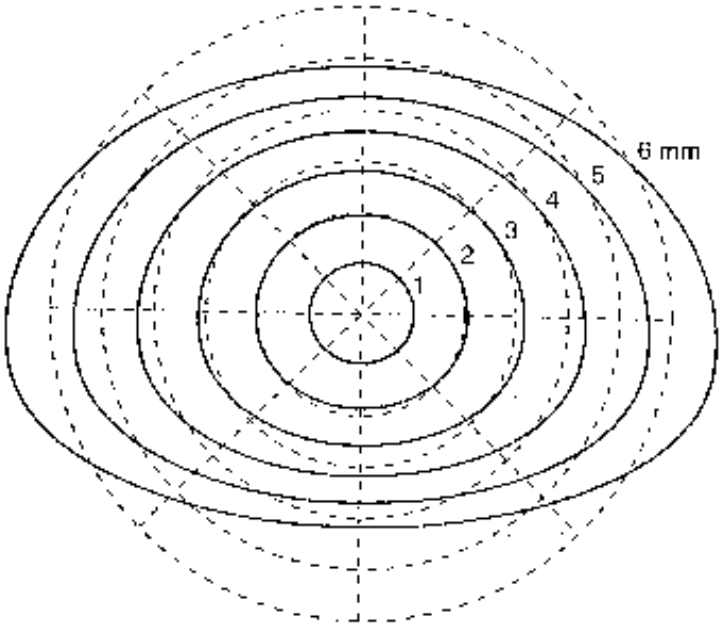

Fig. 3 Equilibrium drop shapes for drop diameters of 1-6 mm. From Beard and Chuang (1987).

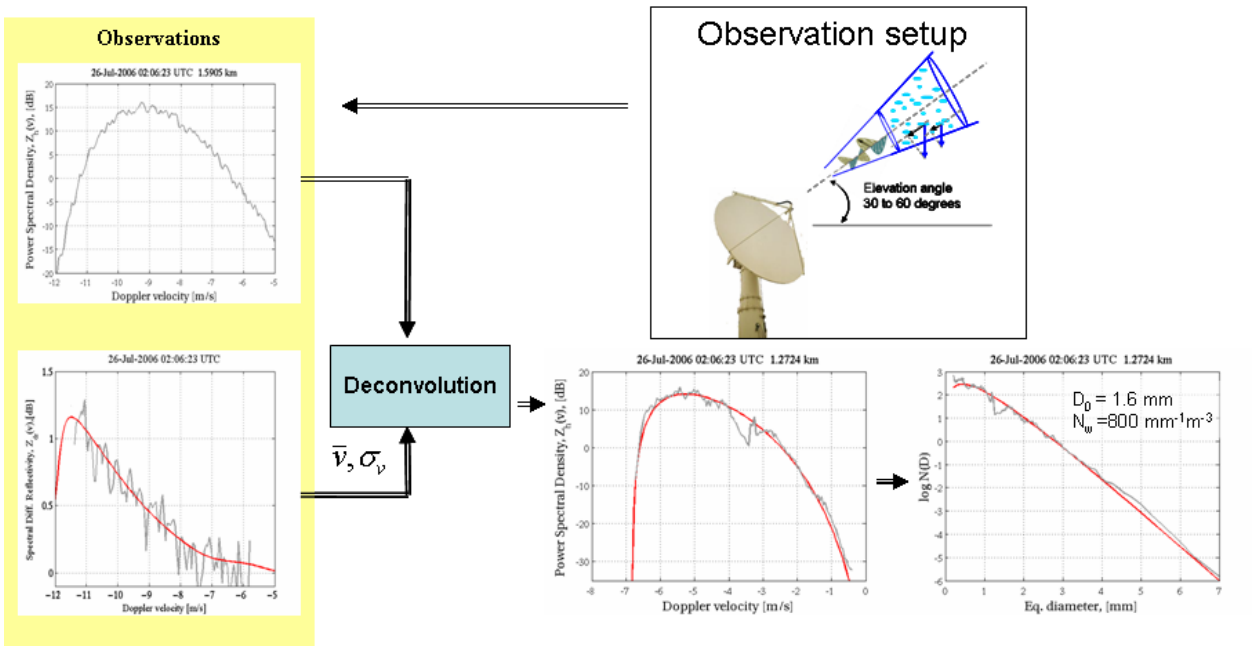

Fig. 4 Block diagram of non-parametric DSD estimation process. Spectral differential reflectivity is used to estimate radial projection of ambient air velocity and spectral broadening kernel width (Moisseev and Chandrasekar, 2007). Then using this information deconvolution procedure applied to the observed Doppler power spectrum. The deconvolved spectrum can be directly be related to a DSD and yields estimated DSD. In the figure above the grey solid lines show measurements, the red lines give best fit to the data.

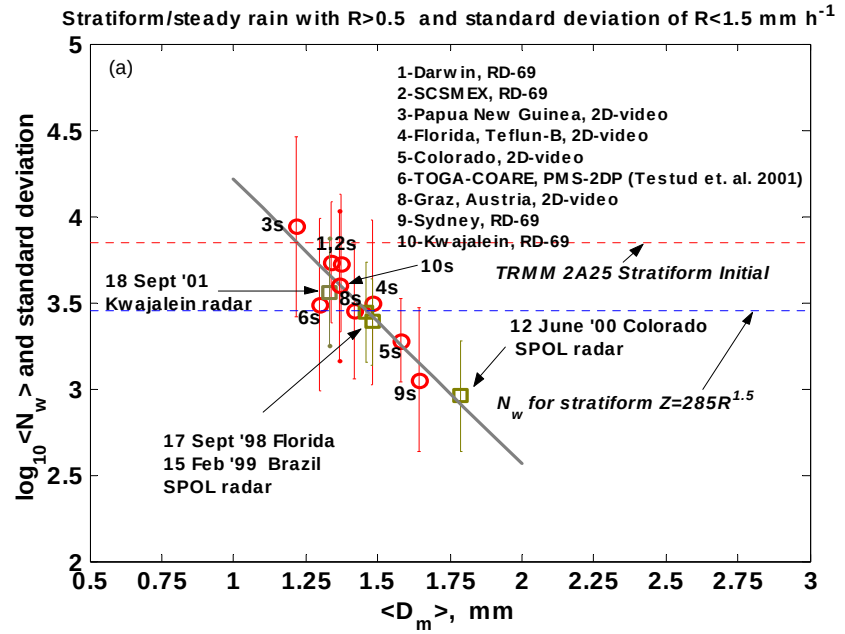

(a)

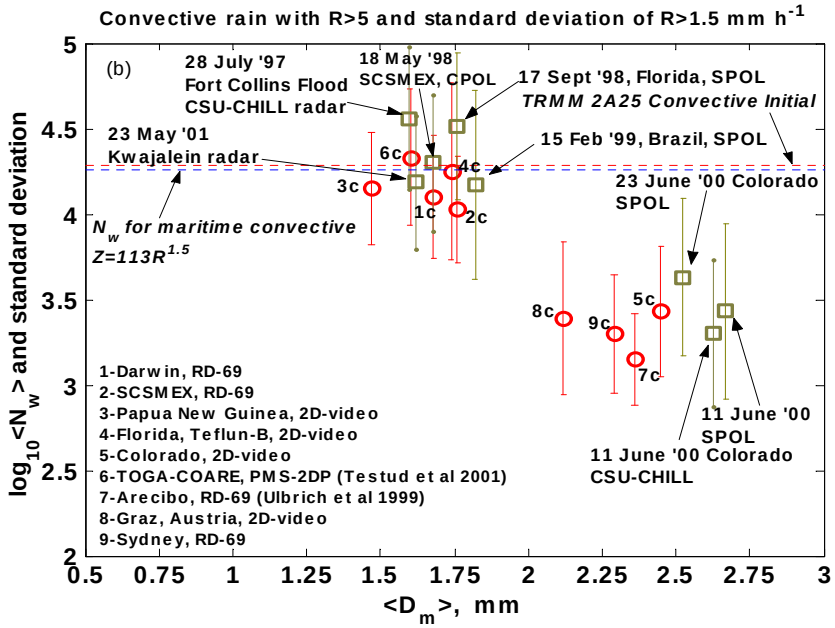

(b)

Fig. 5 The average value of $\log_{10}(N_w)$ (with $\pm 1\sigma$ standard deviation bars) versus average D_m from disdrometer data and radar retrievals as indicated for (a) stratiform rain, and (b) convective rain. Also, the blue dashed horizontal lines at constant $\log_{10}(N_w)$ are the values used for stratiform and convective fixed Z-R relations, while the red dashed ones are derived from TRMM 2A25 initial values. Note that the unit of N_w in this figure is $mm^{-1}m^{-3}$.

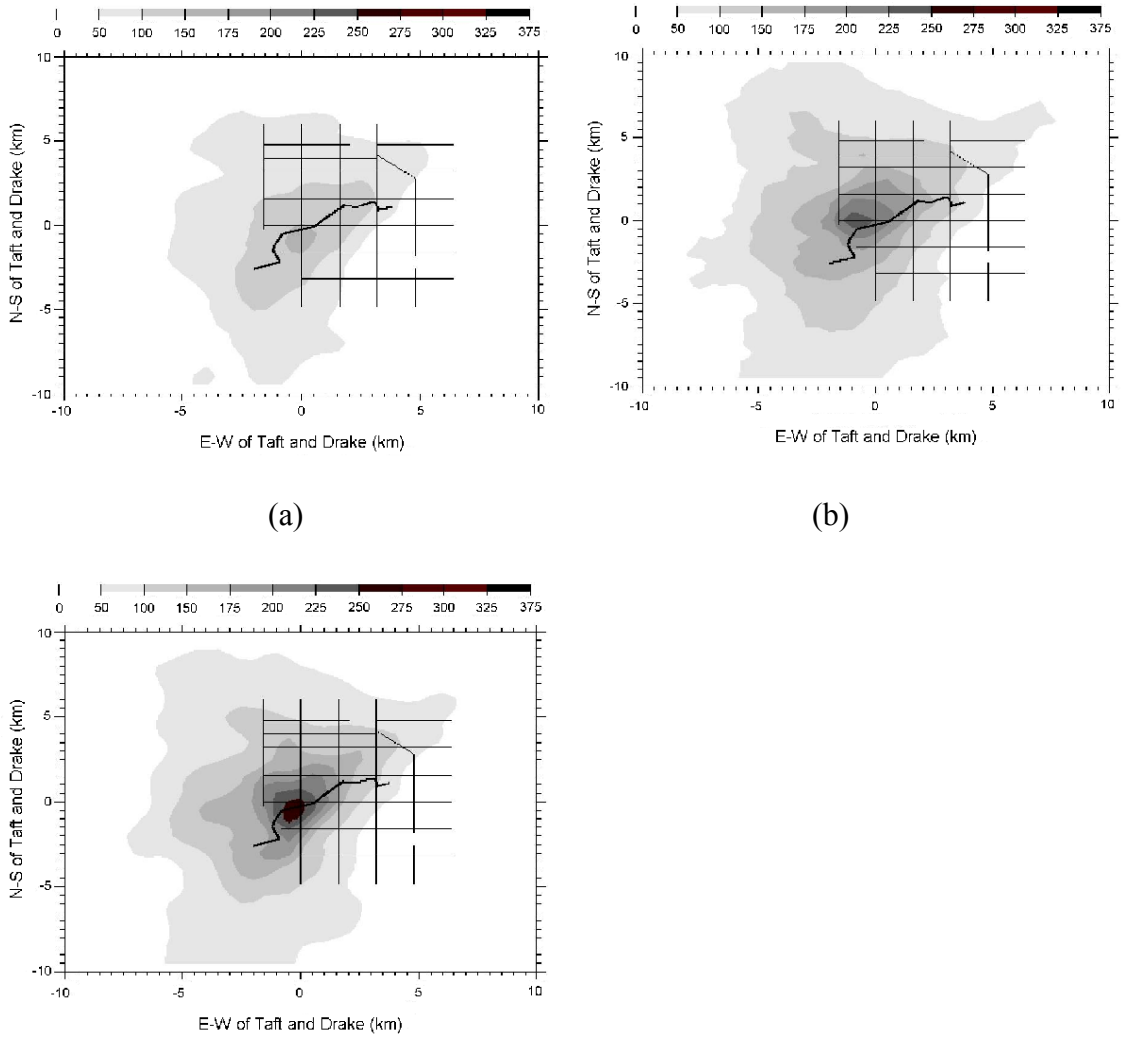

Fig. 6 Storm total rainfall in mm from 17:30 to 22:15 hours MDT. The lines on the picture indicate the street map of the city of Fort Collins. The dark line shows the Spring Creek, which flooded and caused the flash food. (a) $R_{WSR}(Z)$ estimate, (b) $R(K_{dp}, Z_{dr})$ estimate, and (c) $R(Z_h, Z_{dr})$ estimate: (Peterson et al., 1999).

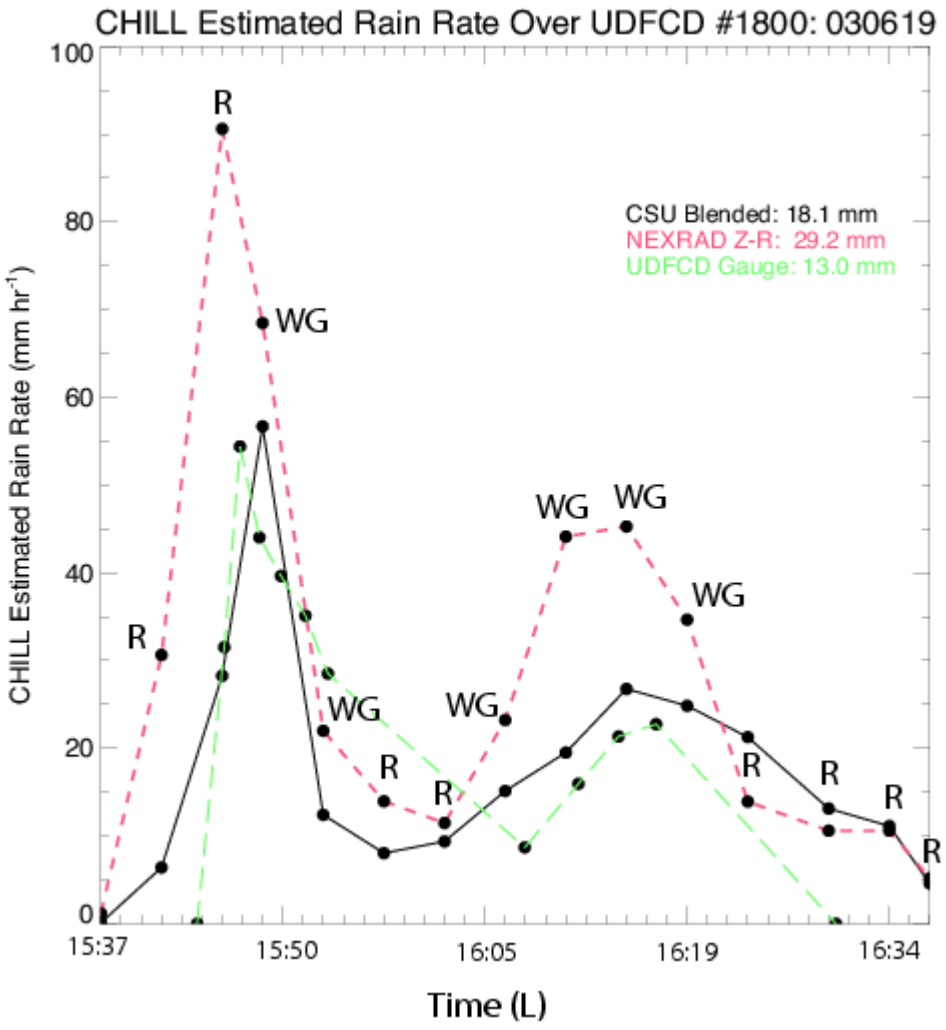

Fig. 7 A time-series of rainfall over the location of the Urban Drainage and Flood Control District (UDFCD) ALERT rain gauge, located near Denver International Airport, on June 19, 2004

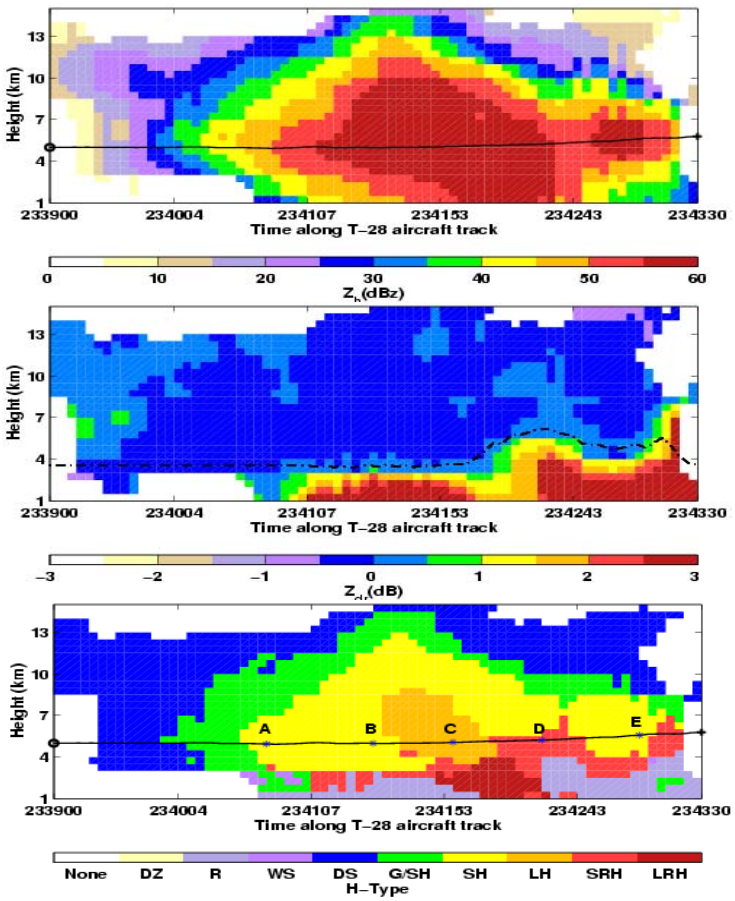

Fig. 8 Vertical structure of radar measurements (Z_h, Z_{dr}) and the hydrometeor classification result corresponding to the case of June 29, 2000. The vertical section data are generated from about 5 minutes PPI volume scan observed by CSU-CHILL radar during Severe Thunderstorm Electrification and Precipitation Study (STEPS). Dotted line in Z_{dr} field is the detected melting level using vertical profiles of Z_h and Z_{dr}.

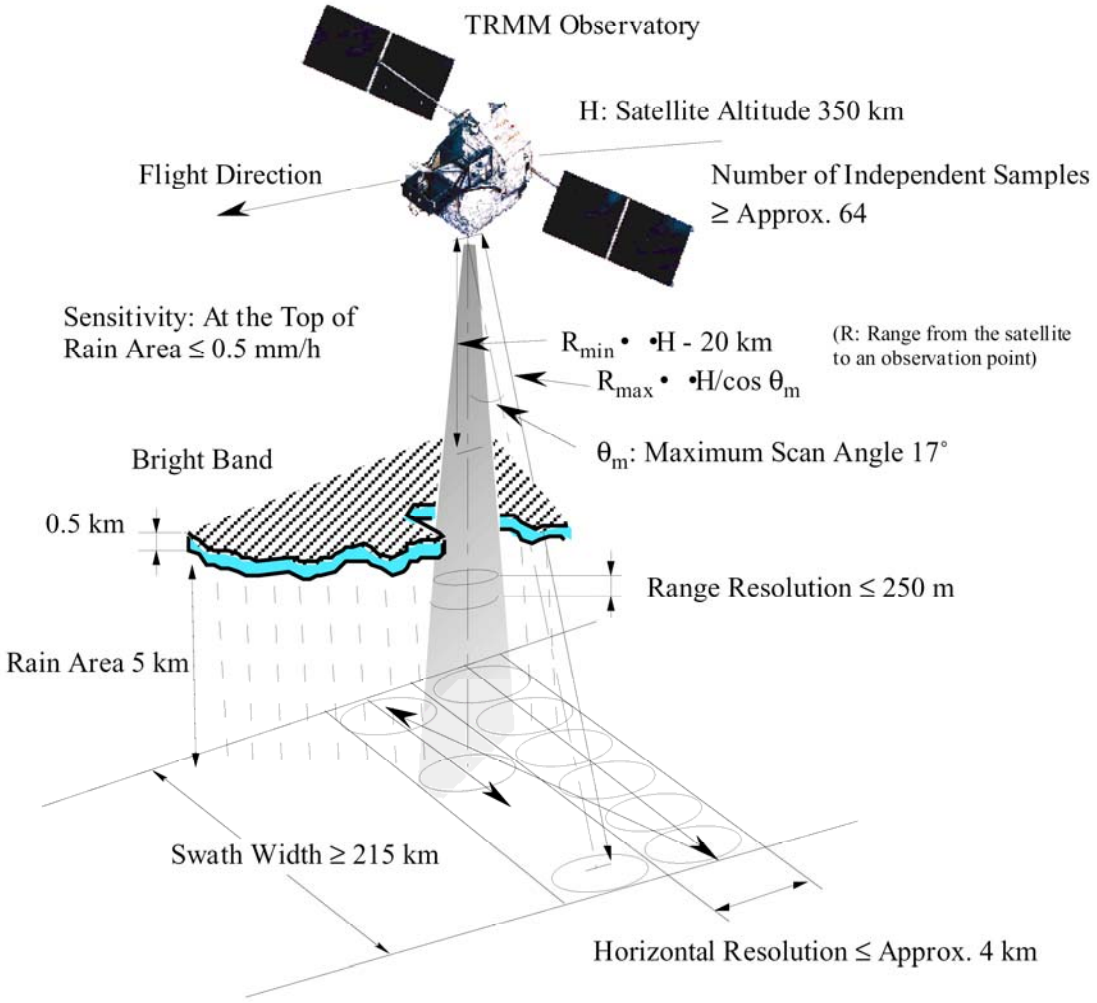

Fig. 9. The observation concept of the PR (adopted from PR Instruction Manual).

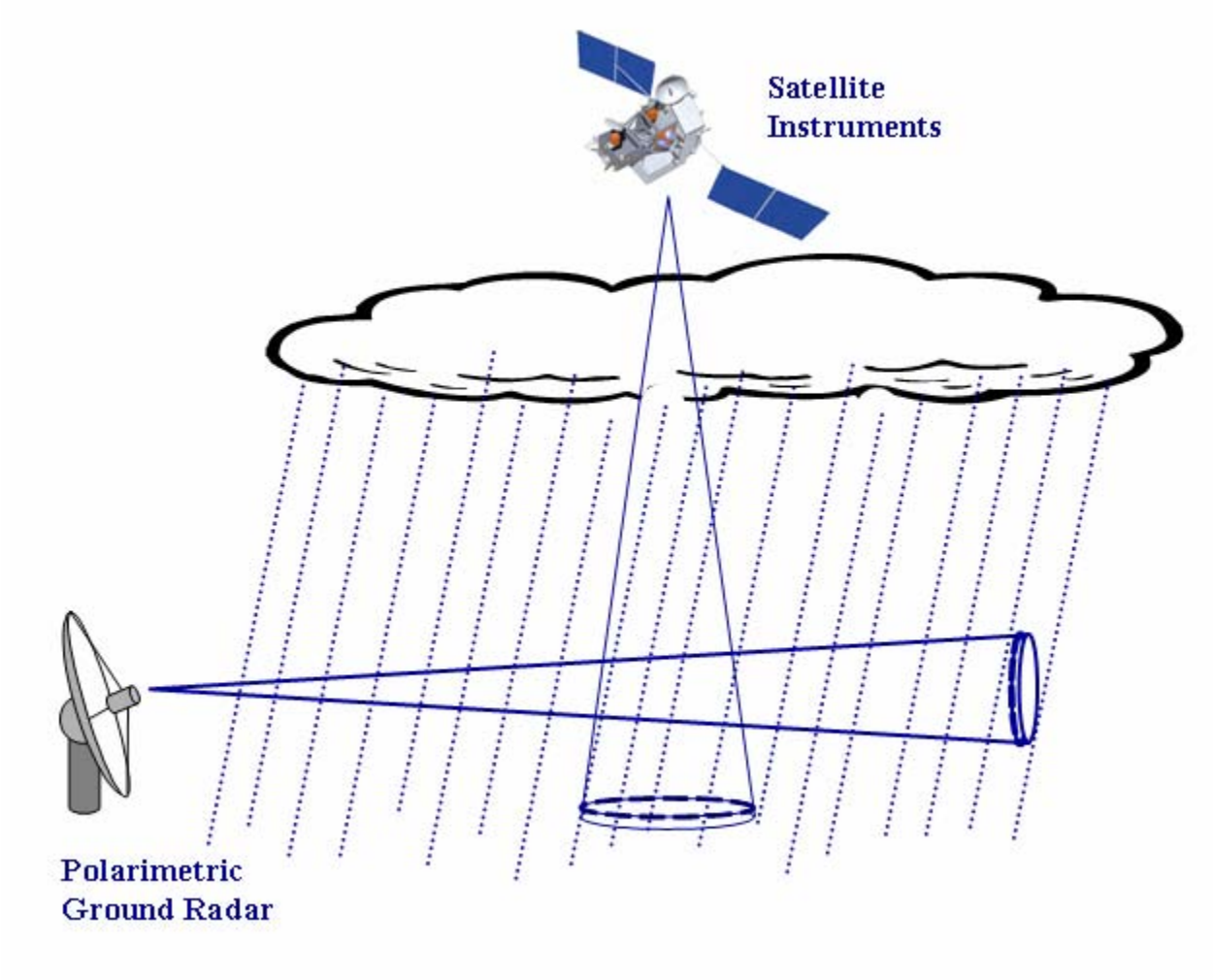

Fig. 10 The schematic of comparing space borne and ground based radar observations.

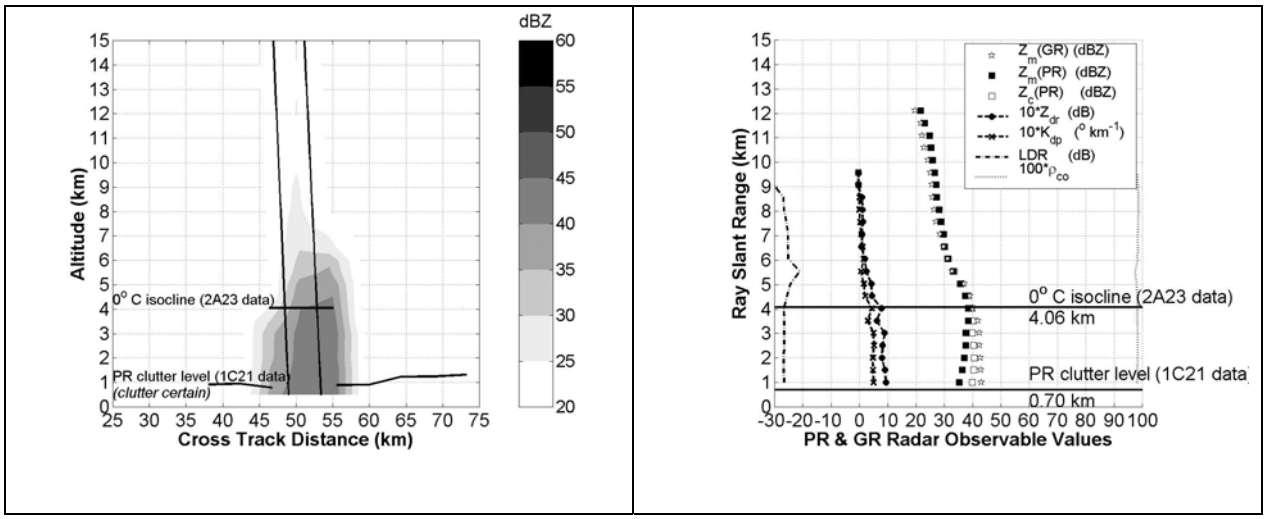

(a) (b)

Fig. 11 Example of ground based observations and RSD estimates from data using TRMM-LBA storm cell A. (a) Vertical profile of GR reflectivity with location of PR beam indicated by solid vertical lines drawn to scale. (b) GR polarimetric observations along PR ray corresponding to the ray as indicated in panel (a). From left to right, the dashed line is LDR, solid line with x's is K_{dp} (scaled by a factor of 10), solid line with circles is Z_{dr} (scaled by 10), black squares are PR measured (attenuated) reflectivity, white squares are PR attenuation corrected reflectivity, stars are GR measured reflectivity and the dotted line is the cross-correlation coefficient between GR return signal horizontal and vertical polarization states, ρ_{co} (scaled by 100). In this plot, PR attenuation is observed to be about 7 dB with reference to GR measurements. In all panels, solid horizontal lines indicate the 0^o C isocline altitude and the PR clutter level (certain), as derived from the TRMM data products, respectively.

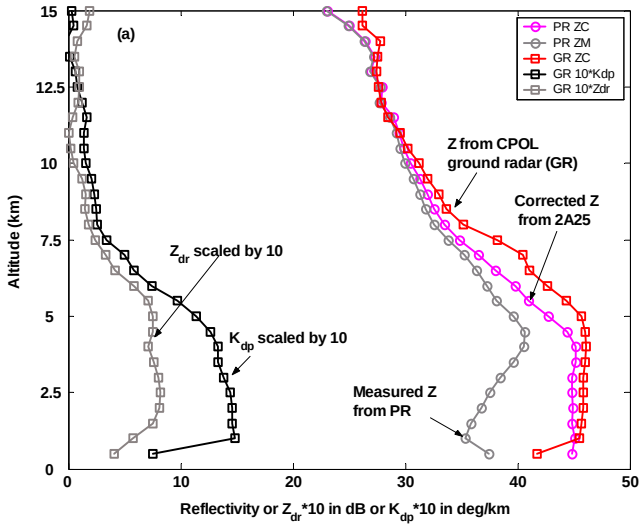

Fig. 12 The (horizontally averaged) vertical profile of measured and corrected reflectivity from PR along with Z_h, Z_{dr} and K_{dp} from the CPOL ground radar (GR). These data are for the Darwin ocean event of 3 February, 2000. The Z match is quite good; it can be noted that average Z_{dr} in the lower rain layer is around 0.8 dB with K_{dp} reaching 1.5 deg/km indicating, on average, a maritime dsd with larger concentration of relatively smaller-sized.

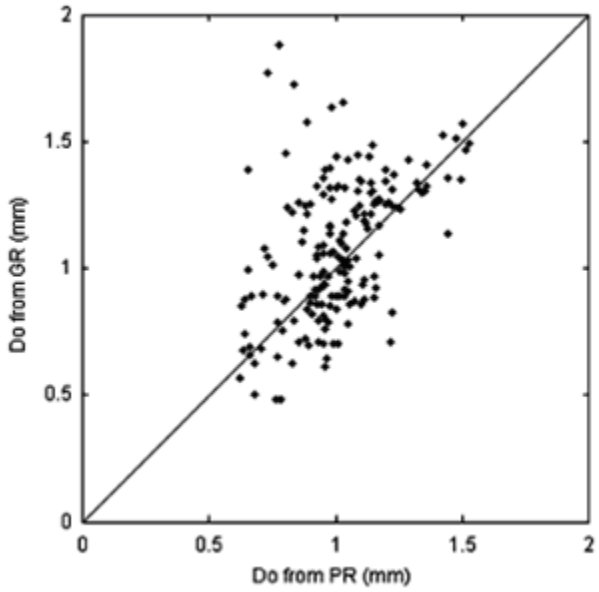

Fig. 13 Scatter plot of D_0 from PR and ground radar for the two cases namely September 18, 1998 and February 25, 1999.